Design and analysis of ultra-wideband decoupling structure based on polarisation mismatch

Jianpu Qiao[1], Weijun Wu[1], Xianliang Zeng[1], Hang Ji[1], and Li Tao[1]

[1]China Ship Development and Design Center

April 18, 2024

Abstract

In this work, a polarization rotating surface is designed and analyzed and applied to the decoupling of ultra-wideband antennas. A method of using dual-size combined rings is proposed to expand the operating bandwidth to 4.8GHz–18.2GHz, and the polarization conversion rate within the entire bandwidth is higher than 99%. Based on the principle of polarization mismatch, placing the polarization rotating surface between ultra-wideband antennas for decoupling can reduce the coupling between antennas by an average of 20dB within the operating bandwidth. Simulation and experimental results consistently prove its excellent decoupling capabilities and ultra-wide operating bandwidth.

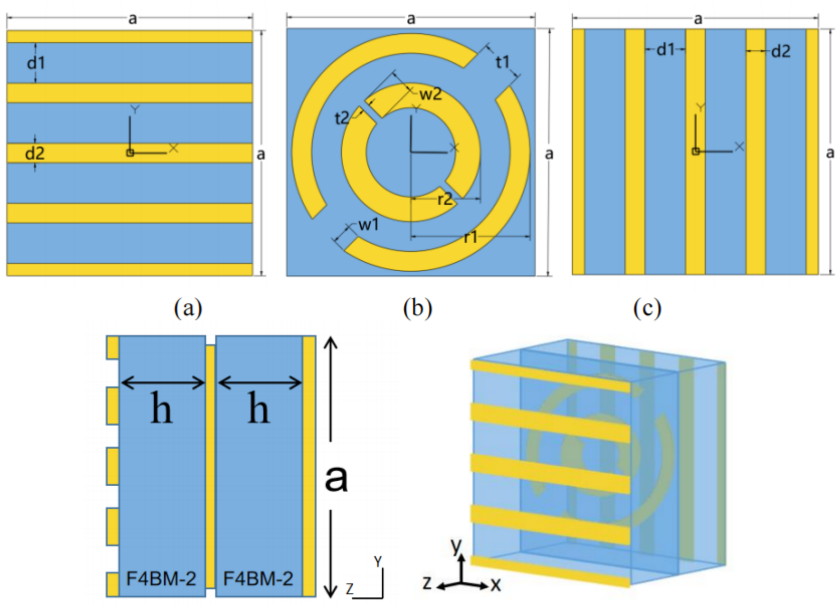

Design and analysis of ultra-wideband decoupling structure based on polarisation mismatch

Jianpu Qiao, Weijun Wu, Xianliang Zeng, Hang Ji,

and Li Tao*

Science and Technology on Electromagnetic Compatibility Laborat-ory, China Ship Development and Design Centre, Wuhan, China

*Email: tl0930@163.com.

In this work, a polarization rotating surface is designed and analyzed and applied to the decoupling of ultra-wideband antennas. A method of using dual-size combined rings is proposed to expand the operating bandwidth to 4.8GHz˜18.2GHz, and the polarization conversion rate within the entire bandwidth is higher than 99%. Based on the principle of polarization mismatch, placing the polarization rotating surface between ultra-wideband antennas for decoupling can reduce the coupling between antennas by an average of 20dB within the operating bandwidth. Simulation and experimental results consistently prove its excellent decoupling capabilities and ultra-wide operating bandwidth.

Introduction: With the development of wireless communication technology, the problem of performance degradation caused by mutual electromagnetic coupling of antennas has attracted more and more attention. At the same time, metamaterials have developed rapidly in just a dozen years due to their special electromagnetic properties that are not found in various natural materials [1-3]. Flexible design of the structure of metamaterials can achieve the control of key characteristic parameters such as amplitude, phase, frequency, and polarisation of electromagnetic waves [4]. However, there are few papers on the application of inter-antenna decoupling from the polarisation dimension. Therefore, it is of great significance to study the decoupling structure between antennas based on the polarisation dimension.

The electromagnetic coupling between antennas mainly consists of three parts: surface waves, coupling between feeders, and space waves [5]. Traditionally, decoupling networks [6], defective ground structures [7], parasitic structures [8] and other methods can be used to decouple between antennas. However, the existence of these technologies affects the antenna radiation characteristics, or the operating bandwidth is not wide enough, or the decoupling effect is average. Therefore, metamaterials with unique properties are used to solve such problems. Many papers apply metamaterials to decoupling between antennas. For example: [9] proposed an effective method to use waveguide metamaterials to suppress the mutual coupling between microstrip patch antennas, reducing the coupling within the operating bandwidth of 6dB. [10] used metamaterial isolators to study the decoupling problem of broadband circularly polarized conformal arrays, and improved the mutual coupling of conformal array antennas in the 3.9GHz˜5.05GHz frequency band. Both structures perform electromagnetic decoupling by blocking electromagnetic propagation between antenna elements. Reducing electromagnetic coupling can also neutralize coupling by providing an additional coupling path. For example, the decoupling surface used in [11] uses metamaterial structure reflection to introduce a new interference path to achieve the same amplitude and anti-phase cancellation. [12] proposed a decoupling structure with polarisation rotation characteristics to reduce the mutual coupling between co-polarized or cross-polarized antennas. It can be seen from the above papers that although many structures in the existing research have good decoupling characteristics, in essence, most of them are considered from the perspective of reducing the amplitude of antenna radiation. According to the electromagnetic wave theory, in addition to the characteristics of amplitude, phase, and frequency, electromagnetic waves also have the basic characteristic of polarisation. This requires mentioning metamaterials with polarisation conversion properties.

The polarisation rotation surface shows excellent properties in polarization conversion and can be considered to reduce electromagnetic coupling between antennas. In [13], an effective technology to reduce the mutual coupling between millimeter-wave dielectric resonator antennas using a new metamaterial polarisation rotator was studied and proposed, ultimately reducing the coupling between antennas by 16dB in the 57˜64GHz frequency band. However, its working bandwidth is narrow, with a relative bandwidth of only 11.57%.

This paper proposes a Polarized Rotating Surface (PRS) in which the middle layer is composed of two orthogonal open resonant rings of different sizes, which is also an innovation of this structure. This structure can convert TE/TM waves into TM/TE waves orthogonal to them, and the polarisation conversion efficiency remains above 99% within the bandwidth. Therefore, the decoupling method of this structure is different from the traditional decoupling by blocking electromagnetic wave propagation, and different from the introduction of additional paths for neutralization and decoupling. Instead, polarisation isolation is achieved by converting electromagnetic waves into their orthogonal waves. Not only that, through electromagnetic simulation, the proposed polarisation rotating surface can reduce the electromagnetic coupling between two ultra-wideband horn antennas whose centers are 1 m apart in the range of 5GHz ˜19GHz by an average of 20dB and a maximum of 30dB. The final experimental results demonstrate that, within the operating frequency band, this PRS can reduce the coupling between ultra- wideband array antennas by an average of 20dB.

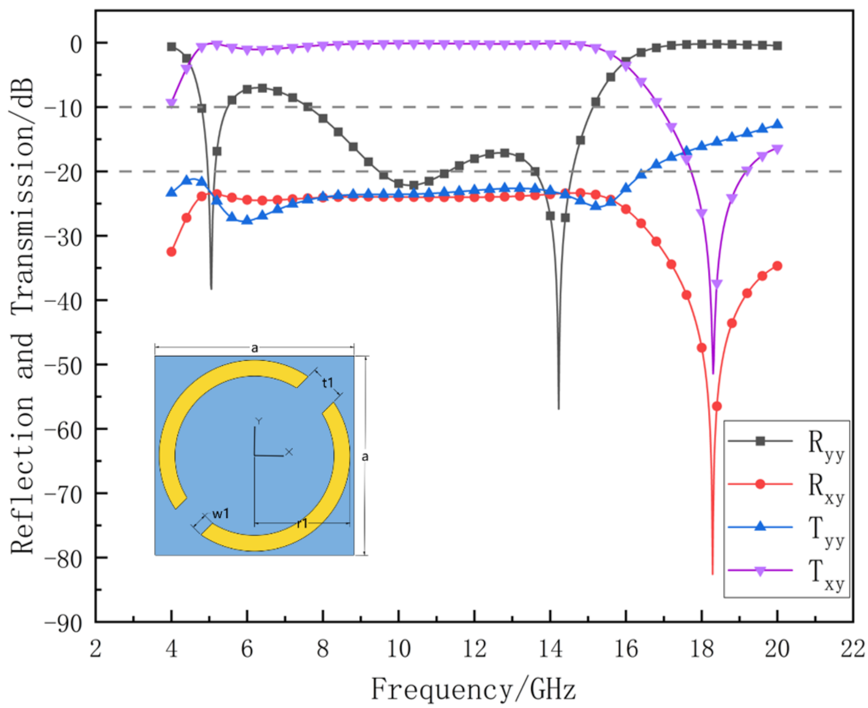

Structural design: Transmissive polarisation converters usually consist of a three-layer structure of a resonant structure array and two layers of orthogonal metal wire grids above and below it [14]. This structure is often called a quasi Fabry–Pérot-like cavity resonant unit structure. The F-P cavity resonant unit structure can cause electromagnetic waves to be reflected multiple times between multi-layer dielectric plates and ultimately increase the amplitude of the transmission coefficient. The metal wire grid can select electromagnetic waves with different polarisation directions. Because the current direction on the surface of the wire grid is distributed along its direction, and the direction of the current on the metal surface is perpendicular to the electric field in the space near it, only when the polarisation direction of the planar electromagnetic wave is perpendicular to the metal wire grid can it pass through the metal wire grid.

The unit structure and specific structural parameters of the PRS in this paper are shown in Figure 1. The unit is divided into three layers. The front and rear are composed of orthogonal metal wire grids. In the middle are two open resonant rings. It is worth noting that the two resonant rings have different sizes and the opening directions are orthogonal to each other. The three layers of metal are separated by two dielectric layers. The metal patch is copper with a thickness of 0.018mm, the conductivity is 5.8×10-7 S/m, the material of the dielectric layer is F4BM-2, the relative dielectric constant is 2.2, and the loss tangent is 0.0015. Among them, the period of the unit is a, the metal wire grid spacing is d1, the metal wire grid width is d2, the outer diameters of the two middle open resonant rings are r1 and r2, the ring widths are w1 and w2, and the opening sizes are t1 and t2, the thickness of both dielectric layers is h.

Simulation results and analysis: When the polarisation direction of the incident electromagnetic wave (y-polarisation) is perpendicular to the metal wire grid, periodic boundary conditions are used to simulate the unit of the polarized rotating surface. The S parameters of the polarisation rotation unit are shown in Figure 2. When there is only a larger double-opening resonant ring in the middle layer of the polarisation rotating surface, the operating bandwidth is 8GHz ˜15GHz, and the relative bandwidth is 60.87%. When there is only a smaller double-opening resonant ring in the middle layer of the polarized rotating surface, the operating bandwidth is 16GHz ˜ 18GHz, and the relative bandwidth is 11.76%. But when the two sizes of double-open resonant rings are placed orthogonally, as shown in the figure, the operating bandwidth is 4.8GHz ˜18.2GHz, and the relative bandwidth is 116.5%. Through the combination of double-open resonant rings of different sizes, the structure can finally work effectively in an ultra-wide frequency band. It is worth noting that in Figure 2 (c), the two sizes of rings must be placed orthogonal to reduce coupling between the two rings.

The surface current distribution on the open resonant ring is shown in Figure 3. At 6GHz, the current is fully coupled to the large loop, indicating that at low frequencies, the polarisation conversion function is mainly carried out by the large loop, and the small loop is almost ineffective; At 12GHz, the surface current is mainly concentrated on the large ring, and there is also partial coupling on the small ring. At this time, the large and small rings work together, but rely more on the large ring to complete polarisation conversion; At 18GHz, the surface current on the small ring is higher, indicating that at high frequencies, the polarisation conversion work is mainly carried out by the small ring. The comparison of surface currents on these three double open resonant rings confirms the reason why the polarized rotating surface designed in this paper can operate in an ultra-wide frequency band.

The efficiency of polarisation rotation can provide an intuitive description of the performance of polarisation converters. Polarisation rotation efficiency (PRE), also known as polarisation conversion rate (PCR), is defined as the ratio of the transmitted cross-polarized electromagnetic wave energy to the total transmitted energy [15]. When the incident electromagnetic wave is y-polarized, the calculation formula for PCR is:

In the formula, 'T' represents the transmitted wave, and the subscript 'xy' represents that the electromagnetic wave is incident by the y-polarized wave and transmitted by the x-polarized wave.

The advantages of the dual-size combination ring designed in this article can also be demonstrated through PCR. From Figure 4, it can be intuitively seen that the performance effect of the polarized rotating surface can convert incident electromagnetic waves into their cross-polarized waves in the range of 4.8GHz˜18.2GHz, with a conversion efficiency higher than 99%. At the same time, when only a small or large ring exists, only a portion of that frequency band can be covered. It is interesting that the two PCR curves in the figure coincidentally intersect and converge at the 16GHz frequency point, which makes people marvel at the ingenuity of the dual size combination ring design.

Comparison of the proposed PRS with the existing PRS is given in Table 2. The superiority of the proposed PRS is strongly demonstrated by its relative bandwidth, PCR, and relative maximum wavelength thickness.

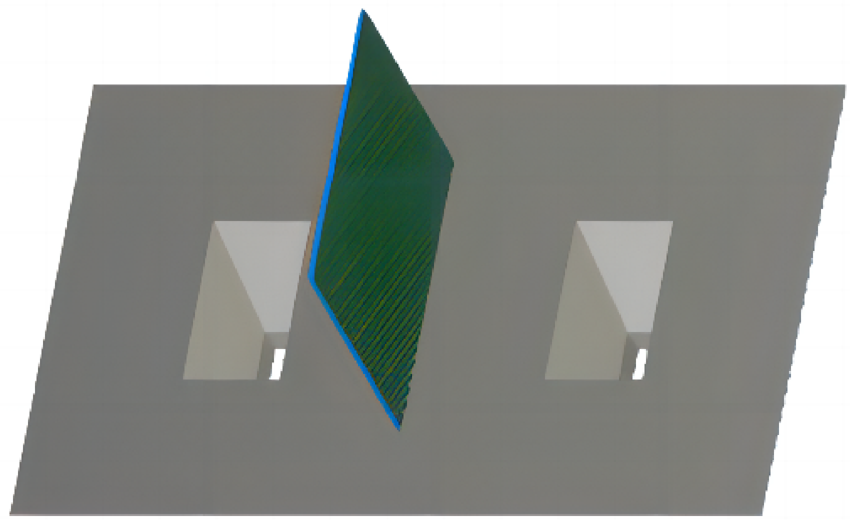

Experimental verification: As is well known, vertically polarized waves need to be received by antennas with vertical polarisation characteristics, while horizontally polarized waves need to be received by antennas with horizontal polarisation characteristics. When the polarisation direction of the incident wave is inconsistent with that of the receiving antenna, the received signal energy will decrease, which means polarisation loss will occur. When the polarisation direction of the receiving antenna is completely orthogonal to the polarisation direction of the incident wave, for example, if a horizontally polarized antenna is used to receive a vertically polarized incident wave, the antenna will not receive the energy of the incident wave at all. In this case, the polarisation loss is the maximum, which is called complete polarisation isolation [16]. This section conducts experiments based on the principle of polarisation mismatch.

Considering the issue of excessive computational complexity and long simulation time when simulating array antennas, we used the horn antenna as the ultra-wideband antenna for simulation. The simulation diagram and simulation results are shown in Figure 5. Over the entire operating frequency range, when PRS is placed between two horn antennas, the coupling between the antennas decreases by an average of 20dB. From the simulation results, it has been proven that the use of polarisation mismatch principle for antenna decoupling is effective, and it has also demonstrated the decoupling ability of the PRS designed in this paper in ultra-wideband.

The processed sample is shown in Figure 6 (b), with a length and width of 400mm and a thickness of 6mm. The medium is the F4BM-2 sheet with a relative dielectric constant of 2.2. This experiment was conducted using the free space method. The experimental scene is shown in Figure 6 (a). The polarisation rotating surface is placed between coplanar array antennas spaced 1m apart. Since a single pair of array antennas cannot cover the entire frequency band, the experiment is divided into two frequency bands: 6GHz ˜ 12GHz and 12GHz ˜ 18GH. For the same reason, the experimental results are also divided into two parts. Figure 7 is a schematic diagram of the coupling comparison between array antennas before and after simulated PRS. In the entire frequency band from 6GHz to 18GHz, PRS can reduce the coupling of the array antenna by an average of 20dB. Since the antennas used in the simulation are different from those used in the experiment, the result curves are also inconsistent. However, from the perspective of decoupling capability and decoupling bandwidth, it is very consistent with the simulation results, which effectively proves the decoupling capability of PRS between ultra-wideband antennas.

Conclusion: Based on the principle of polarisation mismatch, a PRS with polarisation conversion rate higher than 99% was designed and manufactured from the perspective of polarisation. Moreover, the dual-size combined ring is cleverly used to extend the operating bandwidth to an ultra-wide frequency band of 4.8GHz˜18.2GHz. In this paper, the PRS is applied between the ultra-wideband horn antenna and the array antenna. The simulation and experimental results consistently prove its superior performance in decoupling capability and operating bandwidth. In short, this PRS provides a new perspective and method on how to decouple ultra-wideband antennas.

References

1 Pendry J B, Holden A J, Robbins D J, et al. Magnetism from conductors and enhanced nonlinear phenomena[J]. IEEE transactions on microwave theory and techniques, 1999, 47(11): 2075-2084.

2 Xu H X. Research on the Mechanism of Metasurface Electromagnetic Regulation and the Application of Functional Devices[M]. Beijing: Science Press,2019:3-14

3 Wang G M, Cai T, Liang J G, et al. Design and Application of Electromagnetic Superstructured Surface[M]. Beijing: National Defense Industry Press,2020:2-15

4 Cui T J, Li L, Liu S, et al. Information metamaterial systems[J]. Iscience, 2020, 23(8): 101403.

5 He Y, Pan Z, Cheng X, et al. A novel dual-band, dual-polarized, miniaturized and low-profile base station antenna[J]. IEEE Transactions on Antennas and Propagation, 2015, 63(12): 5399-5408.

6 Zou X J, Wang G M, Wang Y W, et al. An efficient decoupling network between feeding points for multielement linear arrays[J]. IEEE Transactions on Antennas and Propagation, 2019, 67(5): 3101-3108.

7 Gao D, Cao Z X, Fu S D, et al. A novel slot-array defected ground structure for decoupling microstrip antenna array[J]. IEEE Transactions on Antennas and Propagation, 2020, 68(10): 7027-7038

8 Li M, Jiang L, Yeung K L. Novel and efficient parasitic decoupling network for closely coupled antennas[J]. IEEE Transactions on Antennas and Propagation, 2019, 67(6): 3574-3585.

9 Yang X M, Liu X G, Zhou X Y, et al. Reduction of mutual coupling between closely packed patch antennas using waveguided metamaterials[J]. IEEE Antennas and Wireless Propagation Letters, 2012, 11: 389-391.

10 Yang F, Peng L, Liao X, et al. Coupling reduction for a wideband circularly polarized conformal array antenna with a single-negative structure[J]. IEEE Antennas and Wireless Propagation Letters, 2019, 18(5): 991-995.

11 Niu Z, Zhang H, Chen Q, et al. Isolation enhancement in closely coupled dual-band MIMO patch antennas[J]. IEEE Antennas and Wireless Propagation Letters, 2019, 18(8): 1686-1690.

12 Liu B, Chen X, Tang J, et al. Co-and cross-polarization decoupling structure with polarization rotation property between linearly polarized dipole antennas with application to decoupling of circularly polarized antennas[J]. IEEE Transactions on Antennas and Propagation, 2022, 70(1): 702-707.

13 Farahani M, Pourahmadazar J, Akbari M, et al. Mutual coupling reduction in millimeter-wave MIMO antenna array using a metamaterial polarization-rotator wall[J]. IEEE Antennas and Wireless Propagation Letters, 2017, 16: 2324-2327.

14 Grady N K, Heyes J E, Chowdhury D R, et al. Terahertz metamaterials for linear polarization conversion and anomalous refraction[J]. Science, 2013, 340(6138): 1304-1307.

15 Wang J, Shen Z, Wu W. Cavity-based high-efficiency and wideband 90° polarization rotator[J]. Applied Physics Letters, 2016, 109(15): 153504.

16 Jin M T. CST Antenna Simulation and Engineering Design[M]. Beijing: Electronic Industry Press.2014: 89

17 Li Y, Zhang J, Qu S, et al. Ultra-broadband linearly polarization manipulation metamaterial[J]. Electronics Letters, 2014, 50(23): 1658-1660.

18 Saikia M, Ghosh S, Bhattacharyya S, et al. Broadband polarization rotator using multilayered metasurfaces[C]//2015 IEEE Applied Electromagnetics Conference (AEMC). IEEE, 2015: 1-2.

19 X Wu, Application research based on metamaterial electromagnetic wave modulation [D] Chongqing University, 2017.

20 Omar A A, Shen Z, Ho S Y. Multiband and wideband 90° polarization rotators[J]. IEEE Antennas and Wireless Propagation Letters, 2018, 17(10): 1822-1826.